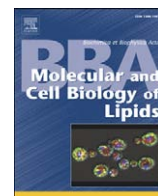


Contents lists available at ScienceDirect

Biochimica et Biophysica Acta

journal homepage: www.elsevier.com/locate/bbalip

Identification of *cis*-acting promoter sequences required for expression of the glycerol-3-phosphate acyltransferase 1 gene in mice

Masaki Yoshida^a, Nagakatsu Harada^{a,*}, Hironori Yamamoto^b, Yutaka Taketani^b, Tadahiko Nakagawa^a, Yunjie Yin^a, Atsushi Hattori^a, Tomoe Zenitani^a, Sayuri Hara^a, Haruka Yonemoto^a, Aki Nakamura^a, Masayuki Nakano^a, Kazuaki Mawatari^a, Kiyoshi Teshigawara^c, Hidekazu Arai^d, Toshio Hosaka^c, Akira Takahashi^a, Katsuhiko Yoshimoto^e, Yutaka Nakaya^a

^a Department of Nutrition and Metabolism, Institute of Health Biosciences, University of Tokushima Graduate School, 3-18-15, Kuramoto-cho, Tokushima City, 770-8503, Japan

^b Department of Clinical Nutrition, Institute of Health Biosciences, University of Tokushima Graduate School, 3-18-15, Kuramoto-cho, Tokushima City, 770-8503, Japan

^c Clinical Research Center for Diabetes, Tokushima University Medical and Dental Hospital, 2-50-1, Kuramoto-cho, Tokushima City, 770-8503, Japan

^d Laboratory of Clinical Nutrition Management, School of Food and Nutritional Sciences, The University of Shizuoka, 52-1, Yada, Suruga-ku, Shizuoka City, 422-8526, Japan

^e Department of Medical Pharmacology, Institute of Health Biosciences, University of Tokushima Graduate School, 3-18-15, Kuramoto-cho, Tokushima City, 770-8503, Japan

ARTICLE INFO

Article history:

Received 25 July 2008

Received in revised form 24 September 2008

Accepted 30 September 2008

Available online 17 October 2008

Keywords:

Glycerol-3-phosphate acyltransferase

Promoter

Sterol regulatory element-binding protein-1

Upstream stimulating factor-1

Liver

Mouse

ABSTRACT

Glycerol-3-phosphate acyltransferase 1 (GPAT1) is a rate limiting enzyme in *de novo* glycerophospholipid synthesis. The murine GPAT1 promoter sequence (the “classical” sequence) was reported previously. However, the organization of this DNA sequence does not fully match the mouse genome sequences on NCBI/GenBank. Here we have identified net *cis*-acting promoter sequences for the mouse GPAT1 gene: promoter 1a which includes part of the classical sequence and the downstream promoter 1b. Promoter 1a facilitates transcription of two alternative GPAT1 transcript variants, GPAT1-V1 and V2, while promoter 1b produces a third transcript variant, GPAT1-V3. Upstream stimulating factor-1 (USF-1) controlled both promoters whereas sterol regulatory element-binding protein-1 (SREBP-1) exclusively regulated promoter 1a activity *in vitro*. Feeding increased GPAT1-V1 and V2, but not V3 mRNA levels in mouse liver. The obese condition of *db/db* mice did not alter the hepatic expression levels of any of the three GPAT1 variants. Feeding enhanced hepatic mRNA levels, intranuclear protein levels and promoter 1a-binding levels of SREBP-1, but not of USF-1. Thus, promoter 1a was exclusively activated by routine feeding *in vivo*. Our results indicate differential roles of the two promoters in the regulation of hepatic GPAT1 gene expression in mice.

© 2008 Elsevier B.V. All rights reserved.

1. Introduction

Glycerol-3-phosphate acyltransferase (GPAT) acts as a rate limiting enzyme in *de novo* synthesis of triacylglycerol (TAG) and phospholipids [1,2]. GPAT catalyzes the first step in glycerophospholipid synthesis, i.e., it acts at the esterification of glycerol-3-phosphate in the *sn*-1 position with a fatty acyl-CoA to form 1-acylglycerol-3-phosphate (lysophosphatidic acid) [1,2]. Four GPAT isoforms, GPAT1 [3], xGPAT1/GPAT2 [4,5], GPAT3/AGPAT8 [6] and GPAT4/AGPAT6 [7,8], have been identified

in mammals. GPAT1 is localized in the outer mitochondrial membrane and its enzymatic activity can be distinguished from the other three GPAT isoforms by its differential sensitivity to sulfhydryl reagents such as N-ethylmaleimide [2,7]. GPAT1 transcript is ubiquitously expressed in mammalian tissues [9]. However, in most tissues, GPAT1 accounts for less than 10% of total GPAT activity, while in the liver its activity is about 50% of the total [2,10], suggesting a significant role of GPAT1 in liver lipid metabolism.

In rat hepatocytes, exogenous overexpression of GPAT1 results in increased synthesis of diacylglycerol and TAG from fatty acids [11]. Such accumulation of TAG by GPAT1 overexpression has also been demonstrated in non-hepatic cells, including Chinese hamster ovary cells [12]. Experimental studies in laboratory animals also have demonstrated that adenoviral overexpression of GPAT1 in the liver results in hepatic steatosis with high accumulation and secretion of TAG [13], whereas a gene knockout or an RNA-interference (RNAi)-induced knockdown of this gene results in a reduction of TAG levels in the liver [14,15]. In addition, a recent study has clearly shown in rats that overexpression of GPAT1 in the liver induces hepatic and systemic insulin resistance [16]. Thus, we believe that GPAT1 is a good candidate for targeted treatment

Abbreviations: GPAT1, glycerol-3-phosphate acyltransferase 1; USF-1, upstream stimulatory factor-1; SREBP-1, sterol regulatory element-binding protein-1; ORF, open reading frame; 5'-RACE, 5'-Rapid amplification of cDNA ends; siRNA, small interfering RNA; EMSA, Electrophoretic Mobility Shift Assay; ChIP, Chromatin immunoprecipitation; ELISA, Enzyme-Linked Immunosorbent Assay; DMEM, Dulbecco's modified Eagle's medium; PMSF, phenylmethylsulfonyl fluoride; SDS, sodium dodecyl sulfate; TAG, triacylglycerol; SRE, sterol regulatory element; ERR, estrogen receptor response element; LXR, liver X receptor; PPAR- α , peroxisome proliferator-activated receptor- α ; RXR, retinoid X receptor

* Corresponding author. Tel: +81 88 633 9594; fax: +81 88 633 7113.

E-mail address: harada@nutr.med.tokushima-u.ac.jp (N. Harada).

of the excess liver lipid accumulation that is associated with obesity and type 2 diabetes with insulin resistance [17].

The cDNA of GPAT1 was cloned first in mouse [3], which was followed by cloning in rat [18] and human [17]. Hepatic expression of GPAT1 mRNA has been reported to be decreased by fasting while it is increased by feeding or insulin treatment *in vivo* [3]. Obese mice with hyperphagia showed high levels of GPAT activity and protein levels in the liver [11], although it is not clear whether the mRNA levels of GPAT1 specifically were changed in this study.

The mouse GPAT1 gene is located on Chromosome 19 [19]. In 1995, Jerkins et al. reported a promoter sequence for the mouse GPAT1 gene [20]. The authors also demonstrated using 3T3-L1 adipocytes that the promoter region encoding nucleotides –322 bp (corrected as –325 bp in this paper) to +102 (relative to the transcription start site) would contain a responsive sequence to insulin or a high glucose environment [20]. Subsequently, Ericsson et al. [21] found three functional sterol regulatory elements (SREs) in this region and demonstrated a significant upregulation of the promoter's activity by SRE-binding protein-1 (SREBP-1), a critical transcription factor for the transcriptional control of lipogenic genes [22]. An additional study by Griffin et al. has also suggested that binding of an upstream stimulating factor 1 (USF-1) to an E-box-like sequence (CATGTG) in this proximal promoter region plays a role in GPAT1 expression [23]. Thus, this proximal region (325 bp) of the GPAT1 promoter has been implicated in both the nutritional as well as hormonal induction of the GPAT1 gene in the liver [20,23].

The murine GPAT1 promoter sequence (with a putative exon 1 sequence) that was reported previously (the classical sequence) [20] is registered in NCBI/GenBank under accession number U11680. However, our *in silico* analysis that was based on the information from NCBI/GenBank has revealed that U11680 is a chimeric sequence mixed with DNA sequence from Chromosome 8, and that the sequence lacked two long intron sequences within the putative exon 1 sequence, although the above-mentioned promoter sequence encoding nucleotides –325 to +102 remained intact. We also found that one of the two intron sequences which are lost in U11680 encodes a *cis*-acting promoter for expression of an additional GPAT1 transcript variant. This paper reveals the genomic organization, transcriptional activity and the differential regulation of the two net promoter regions of the GPAT1 gene in mice.

2. Materials and methods

2.1. Bioinformatics analysis

BLAST-N searching against the mouse genome (<http://www.ncbi.nlm.nih.gov/genome/seq/BlastGen/BlastGen.cgi?taxid=10090>) was performed to analyze the chromosomal localization and exon/intron organization of the previously reported mouse GPAT1 promoter sequence (NCBI/GenBank accession number U11680) [20].

2.2. Animal experiments

Male *db/db* (obese) mice and *db/m+* (non-obese control) mice at 6 weeks of age were purchased from Charles River Japan (Yokohama, Japan). All animal procedures were performed in accordance with the institutional guidelines of Tokushima University. Mice were housed at a constant room temperature of 23 ± 1 °C with a 12-hour light/dark cycle, and were fed a standard non-purified diet (Oriental Yeast, Tokyo, Japan) with food and water available *ad libitum*. At 8 weeks of age, mice were randomly assigned to one of two groups: a fasted group (48 h) or a fed group with free access to food and water. Following the fasting (or feeding) period, body weight and food intake were measured and blood was collected from the abdominal aorta after surgery under anesthesia with an intraperitoneal injection of pentobarbital (50 mg/kg). Epididymal fat depots were then collected and weighed. Blood glucose levels were determined using a glucose sensor (Arkley, Kyoto, Japan). Plasma insulin levels were measured

using an insulin ELISA kit for mice (Shibayagi, Gunma, Japan). Plasma concentrations of TAG, total cholesterol, and free fatty acid were measured using commercial kits (Wako, Osaka, Japan). Liver lipids were extracted by the method of Folch et al. [24] as modified by Drackley et al. [25], and concentrations of total lipid were determined gravimetrically after drying under a stream of nitrogen gas [25]. The lipid extract was redissolved in isopropyl alcohol, and concentrations of TAG were measured by a colorimetric enzymatic procedure using a commercial kit (Wako).

2.3. Cell culture

HepG2 cells and 3T3-L1 preadipocytes were cultured in Dulbecco's modified Eagle's medium (DMEM) containing 10% fetal bovine serum (FBS) and 0.1% gentamycin. In some experiments, the 3T3-L1 preadipocytes were induced to differentiate by changing the medium to DMEM containing 10% FBS, 10 µg/ml insulin, 0.5 mM methylisobutyl-xanthine and 1 µM dexamethasone. After 48 h, this medium was replaced with DMEM supplemented with 10% FBS, and cells were then maintained in this medium for 8 days (medium was changed every 2 days) [4]. Mouse hepatocytes were isolated from male ddY mice (Japan SLC, Shizuoka, Japan) aged 8–10 weeks using the collagenase perfusion method [26], and were then maintained in Williams' medium containing 1 nM insulin, 1 nM dexamethasone, 10% FBS and 0.1% gentamycin.

2.4. Isolation of total RNA and genomic DNA from mouse tissues/cells

Total RNA was extracted from mouse tissues or cultured cells with TRIzol reagent (Invitrogen, Carlsbad, CA). RNA was further purified using an RNeasy kit (QIAGEN, Valencia, CA) before use. Mouse genomic DNA was isolated from the livers of C57BL/6 mice (Japan SLC) using the PUREGENE® Genome DNA Purification kit (Gentra Systems, Minneapolis, MN).

2.5. 5'-Rapid amplification of cDNA ends (RACE)

Amplification of the 5' end of mouse GPAT1 transcripts was performed using the GeneRacer™ Kit (Invitrogen) on liver mRNA isolated from a C57BL/6 mouse. A GeneRacer™ RNA oligonucleotide adaptor (5'-CGACUGGAGCACGAGGACACUGACAUGGACUGAAGGAGUAGAAA-3') was ligated to the 5' end of decapped mRNA using T4 RNA ligase (provided in the kit). First strand cDNA synthesis was then carried out using random primers (provided in the kit). GPAT1-specific primers, 5'-TGGATGGCTTTGGACTGCTGCTG-3' (nucleotide position +469 to +491 relative to the translation initiation site) and 5'-ATCTGGGTCAACTCCGCAGCCA-3' (nucleotide position +437 to +459 relative to the translation initiation site) and adaptor-specific primers (provided in the kit) were used in the primary and secondary PCR rounds with the Expand High Fidelity^{PLUS} PCR System (Roche Diagnostics, Tokyo, Japan). The resulting PCR products were cloned into the pCR®2.1-TOPO vector of the TOPO TA Cloning Kit (Invitrogen) and the nucleotide sequence of the cDNA fragments (5' of GPAT1-V1, V2, and V3) was confirmed with an ABI PRISM 3100-Avant Genetic Analyzer (Applied Biosystems, Foster, CA) using a BigDye® Terminator v1.1 Cycle Sequencing Kit (Applied Biosystems), following the manufacturer's protocol.

2.6. RT-PCR

Total RNA from mouse tissues or cultured cells was reverse transcribed using the ThermoScript RT-PCR System (Invitrogen). Gene-specific primers for each GPAT1 transcript variant and β-actin (internal standard) (Table 1) were designed to amplify a 199-bp, 172-bp, 196-bp and 510-bp fragment of GPAT1-V1, GPAT1-V2, GPAT1-V3 and β-actin cDNA, respectively. PCR reactions were carried out using Taq DNA Polymerase (New England Biolabs, Inc, Beverly, MA) with the following cycling parameters: 94 °C for 2 min; 35 cycles of 94 °C for 30 s,

Table 1
Primer sets used for PCR

Target	Primer sequence	Localization
GPAT1-V1 (for RT-PCR, qRT-PCR)	F: 5'-CCTGGGGCTGCTCTCTCG-3' R: 5'-CTTTGGCTTGGCTTCTAGG-3'	Exon 1a Exon 1b
GPAT1-V2 (for RT-PCR, qRT-PCR)	F: 5'-GCTGTGACCCGAAGGTCTC-3' R: 5'-CAAACCATGTGTATCCTTG-3'	Exon 1a Exons 1a/1c junction
GPAT1-V3 (for RT-PCR, qRT-PCR)	F: 5'-ATTCCTTTCTCAGAGCCTGG-3' R: 5'-GCAAGTCCAAACCATGTG-3'	See also Fig. 2A Exon 1c
GPAT1-total (for qRT-PCR)	F: 5'-GGAAGGTGCTGTAATCCTG-3' R: 5'-CATCCTCTGTGCCTGTGTG-3'	Exon 3 Exons 4/5 junction
SREBP-1c (for qRT-PCR)	F: 5'-GGAGCCATGGATTGCACATT-3' R: 5'-AGAGGAGGCCAGAGAAGCAGA-3'	
USF-1 (for qRT-PCR)	F: 5'-ACGCTTCCGAAGTGAATGG-3' R: 5'-GGTGAAGCTCCCTGGATCA-3'	
18S ribosomal RNA (for qRT-PCR)	F: 5'-AAACGGCTACCACATCAAG-3' R: 5'-GGCTCCGAAGAGTCTGTA-3'	
β -actin (for RT-PCR)	F: 5'-GATGACGATATCGCTCGCT-3' R: 5'-TAGATGGCAGACGTGGGT-3'	

F: forward primer, R: reverse primer. qRT-PCR: quantitative RT-PCR.

57–59 °C for 30 s, and 72 °C for 30 s; and a final extension at 72 °C for 7 min. Amplification of the β -actin cDNA fragment was carried out with the same PCR system using the following cycling parameters: 94 °C for 2 min; 28 cycles of 94 °C for 30 s, 56.5 °C for 30 s, and 72 °C for 1 min; and a final extension at 72 °C for 7 min. The PCR products were then electrophoresed on a 1.5% agarose gel.

2.7. Quantitative real-time RT-PCR

Total RNA isolated from the liver of *db/db* or *db/m+* mouse or primary cultured hepatocytes was reverse transcribed using TaKaRa PrimeScript[®] RT reagent kits (TaKaRa, Kyoto, Japan). Quantitative real-time PCR was performed with the LightCycler system (Roche Diagnostics) using TaKaRa SYBR Premix Ex Taq (TaKaRa) and the gene-specific primers listed in Table 1. After the reaction, each PCR product was verified for its single amplification by melting curve analysis, and also by agarose gel electrophoresis of the products followed by subcloning into a pCR[®]2.1-TOPO vector (Invitrogen) and nucleotide sequencing as described above. The expression levels were normalized to the expression of 18S ribosomal RNA (see Table 1 for primer sequences) in each sample and are given in arbitrary units.

2.8. Plasmids

A series of 5'-flanking DNA fragments encoding nucleotides -1797, -789, -728, and -325 to +103 of the mouse GPAT1 exon 1a, and -2107, -257, -107, -91, and -20 to +152 of the mouse GPAT1 exon 1b (relative to the transcription start site) was generated by PCR using C57BL/6 mouse genomic DNA and the specific primers listed in supplementary Table S1. PCR products were subcloned with the TOPO TA Cloning Kit (Invitrogen), and the nucleotide sequence of each DNA fragment was confirmed as described above. Each DNA insert was isolated with restriction enzymes (supplementary Table S1), and inserted into the same restriction sites of the pGL3-basic luciferase reporter vector (Promega, Madison, WI), generating PGL 1a (-1797), (-789), (-728), (-325) and PGL 1b (-2107), (-257), (-107), (-91) and (-20). PGL 1a (-86) was constructed by digesting PGL 1a (-1797) plasmid with Hind III, and inserting the fragment into the Hind III site of the pGL3-basic vector. PGL 1b (-809) was generated by cutting out a 1.3-kb Sac I fragment from the PGL 1b (-2107) plasmid, followed by self-ligating the remaining fragment at the Sac I site. PGL 1b (-458) was constructed by cutting out a 1.65-kb fragment from the PGL 1b (-2107) plasmid with Nhe I and Bln I (both generate a 5'-CTAG extension), and self-ligating the remaining fragment at the 5'-CTAG extension ends. PGL 1b (-257)m1, PGL 1b (-107)m, and PGL 1b (-91)m were constructed by the same method as PGL 1b (-257), PGL 1b (-107), and PGL 1b (-91), respectively, but using the specific mutant (sense)

primers listed in supplementary Table S1. PGL 1b (-257)m2 and PGL 1b (-257)m3 were generated by site-directed mutagenesis [27] using a PGL 1b (-257) plasmid and the PCR primers listed in supplementary Table S1. All plasmids were purified with a plasmid purification kit (QIAGEN) before use.

A mouse GPAT1 cDNA including an open reading frame (ORF) but lacking a translational stop codon in its nucleotide sequence was amplified by RT-PCR using the Expand High Fidelity^{PLUS} PCR System (Roche Diagnostics) on mouse liver RNA. The gene-specific primers used are as follows: forward: 5'-TCTGCCATGGAGGAGTCTTC-3' (translational initiation codon ATG is underlined), reverse: 5'-CAGACCA-CAAACTCAGAATATAC -3'. The PCR product was subcloned using a TOPO TA Cloning[®] Kit (Invitrogen), and the nucleotide sequence of the GPAT1 cDNA fragment was confirmed as described above. A BamHI and Not I double-digested fragment was ligated in frame into the pcDNA3.1/Myc-His (+) vector (Invitrogen), so that the resulting fusion construct encoded a myc epitope plus 6×His tag at the C terminus of GPAT1 (GPAT1-myc). A pCR[®]2.1-TOPO vector containing a 5' fragment of either GPAT1-V1, V2, or V3 (obtained by the 5'-RACE method) (see above) was subjected to PCR with specific forward primers (for GPAT1-V1 and V2: 5'-AAGGATCCACTGTTGCAAAACCATCTGGAC-3', for GPAT1-V3: 5'-AAGGATCCATTCCTTTCTCAGAGCCTGGCAA-3') (BamHI restriction sites are underlined) and the reverse primer [5'-ATCTGGGTCAACTCCGAGCCA-3' (nucleotide position +437 to +459 relative to the translation initiation site)]. The PCR product was subcloned using a TOPO TA Cloning[®] Kit (Invitrogen). A sequence-confirmed DNA fragment was isolated by digestion with BamHI and PshA I (nucleotide position +329 relative to the translation initiation site) and inserted into the same restriction sites of the GPAT1-myc plasmid, generating GPAT1-V1-myc, GPAT1-V2-myc, and GPAT1-V3-myc expression plasmids.

A human SREBP-1c (hSREBP-1c) (a.a. 1-449) expression plasmid (in pcDNA3.1/Myc-His (+) vector) was constructed as described previously [28]. A human SREBP-1c (a.a. 66-449) (termed hSREBP-1-DN) was amplified by PCR by the same method as for hSREBP-1c (1-449), but using a different forward primer: 5'-TCCTGAGCATGCCGAGGCA-3' (designed in exon 2). Note that the 'GG' dinucleotides in the normal sequence were replaced with 'AT' in the primer sequence to form the translation initiation codon ATG (underlined).

A cDNA fragment of human USF-1 (hUSF-1; NCBI/GenBank accession number NM_007122) was amplified by RT-PCR and the PCR product was subcloned using a TOPO TA Cloning[®] Kit (Invitrogen). A sequence-confirmed ORF fragment with (hUSF-1) or without (hUSF-1/BD; a dominant negative form) sequence from exon 4 [29] was isolated by digestion with EcoR I, and inserted into the pcDNA3.1 vector (Invitrogen).

2.9. Coupled transcription/translation

After linearization of an equal amount (1 μ g) of the GPAT1-myc, GPAT1-V1-myc, GPAT1-V2-myc, or GPAT1-V3-myc expression plasmid or empty vector [pcDNA3.1/Myc-His(+)], each GPAT1 protein was synthesized *in vitro* under the control of the T7 promoter using a T_{NT}[®] Quick Coupled Transcription/Translation System (Promega, Madison, WI) at 30 °C for 90 min in the presence of 20 μ M methionine. An hUSF-1 expression plasmid (in pcDNA3.1 vector) (constructed as described above) was also subjected to the same reaction and the generated protein were used for an Electrophoretic Mobility Shift Assay (EMSA) (see below).

2.10. Luciferase assay

HepG2 cells grown in a 24-well plate were transiently transfected with 0.12 μ g of the luciferase reporter plasmid, and 0.06 μ g of either hSREBP-1c (1-449), hSREBP-1-DN, hUSF-1, or hUSF-1/BD expression plasmid using the Lipofectamine[™] and Plus[™] reagents (Invitrogen).

The normalized transfection efficiency for luciferase activity was determined by co-transfecting with 0.06 µg of a β-galactosidase (β-gal) expression vector, pCMV-β (Stratagene, La Jolla, CA). After 48 h, cells were harvested in a lysis buffer supplied with the luciferase assay kit (Promega), and the lysates were assayed for luciferase activity and β-gal activity as described previously [28].

2.11. Transfection of siRNA

Double-stranded RNA duplexes used for knockdown of mouse USF-1 (sc-36784) or mouse SREBP-1 (sc-36558) were purchased from Santa Cruz Biotechnology, Inc. (Santa Cruz, CA). A control RNA duplex with a scrambled sequence (sc-37007) was also obtained from Santa Cruz Biotechnology, Inc. Primary cultures of mouse hepatocytes were transfected with either of these siRNAs using the Lipofectamine 2000 reagent (Invitrogen) [26]. Cells were used 48 h after transfection.

2.12. Extraction of nuclear protein

Extraction of liver nuclear protein was performed as previously reported [30] with some modifications. Mouse liver was homogenized in Buffer A [10 mM Tris–Cl, pH 7.5, 0.25 M sucrose, 3 mM MgCl₂, 1 mM phenylmethylsulfonyl fluoride (PMSF), 4 µg/ml leupeptin, and 4 µg/ml aprotinin] using a Dounce homogenizer with an A-type pestle (10 strokes), followed by centrifugation at 300×g for 5 min at 2 °C. The pellet was resuspended in Buffer A, adjusted to 1% Nonidet P-40, and homogenized. The homogenate was then centrifuged (300×g for 5 min at 2 °C). The nuclear pellet was resuspended in Buffer B (50 mM Hepes, pH 7.4, 0.1 M KCl, 3 mM MgCl₂, 1 mM EDTA, 10% glycerol, 1 mM PMSF, 4 µg/ml leupeptin, and 4 µg/ml aprotinin), and adjusted to 0.4 M ammonium sulfate. The mixture was agitated gently at 4 °C for 40 min, and then centrifuged at 100,000×g for 60 min. The supernatant was used as a nuclear extract.

2.13. Immunoblotting

Equal amounts of the sample proteins were denatured by boiling for 5 min in a sodium dodecyl sulfate (SDS) sample buffer containing 1% β-mercaptoethanol. The proteins were then electrophoresed on an SDS-polyacrylamide gel and transferred onto an Immobilon-P membrane (Millipore, Bedford, MA). The membrane was blocked in 5% skim milk in Tris-buffered saline containing 0.05% Tween 20 for 1 hour and incubated with an anti-*myc* tag rabbit polyclonal antibody (1: 500, Cell Signaling Technology, Inc, MA, USA), anti-USF-1 rabbit polyclonal antibody (1: 1000, Santa Cruz Biotechnology, Inc.), or anti-SREBP-1 rabbit polyclonal antibody (1: 1000, Santa Cruz Biotechnology, Inc.). Proteins were then visualized with an anti-rabbit IgG horseradish peroxidase-conjugated secondary antibody (1:10 000, Biosource International, Camarillo, CA) using an ECL Plus detection kit (Amersham Pharmacia Biotech, Aylesbury, UK).

2.14. EMSA

EMSA was performed as described previously [31]. Double-stranded oligonucleotides corresponding to nucleotides –111 to –88 (oligo. A: 5'-CTTTAGGTACATTCCTGGAC-3'), or –88 to –65 (oligo. B: 5'-CTACTCGGTACAGTATCTTG-3') in the 5'-flanking region of exon 1b (relative to the transcription start site), as well as their mutant sequences; oligo. Am: 5'-CTTTAGATATCATTCCTGGAC-3', and oligo. Bm: 5'-CTACTCGGTTCGATGATCATCTTG-3' were synthesized (mutated positions are underlined). Double-stranded oligonucleotides encoding an E-box positive sequence [32] or a negative sequence (in which the E-box sequence is disrupted) were also synthesized. Purified oligonucleotides were labeled by T4 polynucleotide kinase with [γ -³²P] ATP (>259 TBq/mmol; MP Biomedicals, Irvine, CA). The labeled probes were further purified with MicroSpin™ G-25 Columns (GE Healthcare

UK Ltd., UK) before use. The binding reaction was performed for 30 min at room temperature in a final volume of 20 µl containing 75 mM Tris–HCl, 375 mM NaCl, 7.5 mM EDTA, 7.5 mM dithiothreitol, 37.6% glycerol, 1.5% NP-40, 5 mg/ml BSA, 0.05 mg/ml Poly (dl) Poly (dC), 1 µl of *in vitro* synthesized hUSF-1 protein, and 100 nM of the double-stranded oligonucleotide probe. For the competition assay, unlabeled double-stranded oligonucleotide (10 µM) was added to the binding buffer. The reaction mixture was then electrophoresed on a 5% polyacrylamide gel. The gel was then dried and analyzed with a bioimaging analyzer (BAS-1500, Fuji-film, Tokyo).

2.15. Chromatin immunoprecipitation (ChIP)

A ChIP assay was performed as previously described [33] with some modifications. The liver samples from *db/m+* or *db/db* mice were cross-linked with 1% formaldehyde (in PBS) at room temperature for 15 min. The reaction was terminated by the addition of 125 mM glycine. Crosslinked liver samples were washed once with cold PBS and swelled in RSB buffer [10 mM Tris–HCl (pH 7.4), 3 mM MgCl₂, 10 mM NaCl, 2% NP-40, 1 µg/ml aprotinin, 1 µg/ml leupeptin, and 1 mM PMSF], and then homogenized with a douncer. After centrifugation, pelleted nuclei were washed with RSB buffer and after additional centrifugation, resuspended in nuclear lysis buffer [50 mM Tris–HCl (pH 8.1), 1% SDS, 10 mM EDTA, 1 µg/ml aprotinin, 1 µg/ml leupeptin, and 1 mM PMSF]. The resulting chromatin solution was then sonicated using a MICROSON™ XL2000 sonicator (MISONIX, Farmingdale, NY) for 10×8 s to shear chromatin. Chromatin size was determined by agarose electrophoresis to ensure that the average size was between 200 and 400 bp. After centrifugation, the supernatant was diluted 1:10 in dilution buffer [16.7 mM Tris–HCl (pH 8.1), 0.01% SDS, 1.1% Triton X-100, 1.2 mM EDTA, 150 mM NaCl, and the protease inhibitors]. The diluted samples were pre-cleared with blocked protein A-sepharose (Sigma, St. Louis, MO). Following centrifugation, the supernatants were mixed with 2 µg of anti-USF1 antibody (sc-8983X; Santa Cruz), 2 µg of anti-SREBP-1 antibody (sc-8984; Santa Cruz) that recognizes both 1a and 1c isoforms, or 2 µg of non-immuno rabbit IgG (Santa Cruz) and incubated overnight at 4 °C. Antibody–protein–DNA complexes were isolated by immunoprecipitation with preblocked protein A-sepharose. Following extensive washing, these complexes were eluted with elution buffer (100 mM NaHCO₃, 1% SDS, and 10 mM dithiothreitol). After addition of 0.2 M NaCl, samples were incubated at 65 °C for 4 h to reverse the formaldehyde cross-links. Aliquots of the precleared chromatin solutions without antibody incubation (termed “input”) were also subjected to de-crosslinking during this process. After digestion with RNase A (20 mg/ml, 37 °C, 30 min) and proteinase K (50 mg/ml, 50 °C, 60 min), DNA was extracted from each sample. Purified DNA was subjected to quantitative PCR using the following primers: for the E-box in promoter 1a: 5'-CAAAGTAGACCCAGCCAGACC-3'(sense) and 5'-GGTGTCTTCTGGCTTCGC-3'(antisense); for the estrogen receptor response element (ERR)-like sequence with E-box (E4) in promoter 1b: 5'-CCCTTAACTGGGAGAGCAGAG-3'(sense), and 5'-TTTTGTTTCAGGGTATCTTTGCC-3'(antisense); and for the SRE-like sequence in promoter 1a: 5'-CCAACTACCCAGTGCAG-3'(sense) and 5'-TTGATCAGCCAATCGAAAGC-3'(antisense). The values for non-immuno IgG-immunoprecipitated DNA were subtracted from the values for USF-1 or SREBP-1-immunoprecipitated DNA in each sample. The levels of immunoprecipitated DNA were then normalized to the levels of initial immunoprecipitable DNA (corresponding to the amounts of PCR products in each “input” sample) and are given in arbitrary units.

2.16. Statistical analysis

Data are expressed as the means±SD. Data were analyzed by ANOVA plus Bonferroni multiple comparison tests. A *P*-value<0.05 was considered to be statistically significant.

3. Results

3.1. Genomic organization of the mouse GPAT1 gene

The genomic organization of the mouse GPAT1 gene was analyzed *in silico* using NCBI genome search programs with the previously reported 5'-flanking DNA sequence of the GPAT1 gene (GenBank accession number U11680) [20] as a probe. As shown in Fig. 1A, genome analysis revealed that the DNA region upstream from -428 [relative to the transcriptional initiation site (+1)] of this sequence (termed U11680-upper) was mapped to contigs NT_039457.6, NW_001030892.1 and NW_000339.1, all of which were localized on Chromosome 8. However, the DNA region downstream from -428 (termed U11680-lower) was mapped to contigs of Chromosome 19 (NT_039687.6, NW_001030648.1 and NW_000148.1) (Fig. 1A and B). A GATC sequence was located at the U11680-upper-lower sequence junction (Fig. 1A). An NCBI genome analysis (BLAST Mouse Sequences; <http://www.ncbi.nlm.nih.gov/genome/seq/BlastGen/BlastGen.cgi?taxid=10090>) of the U11680-lower sequence further revealed that the DNA region downstream from +1 must be divided into three putative exon sequences (termed exons 1a, 1b, and 1c). Exons 1a and 1b are located approximately 28 kb and 5 kb, respectively, upstream of exon 1c in the mouse genome (Fig. 1B). An NCBI genome analysis also revealed that all sequences at the exon-intron junctions are consistent with the AG-GT rule (Table 2) [34].

3.2. The mouse GPAT1 gene produces three transcript variants

Previously, Jerkins et al. identified a transcription initiation site of the GPAT1 gene by primer extension analysis using a primer that was complementary to nucleotides +99 to +115 (relative to the transcription start site) [20]. Thus, this primer was located in exon 1a according to our analysis (Fig. 1B). Here we carried out 5'-RACE analysis to obtain the sequence of the 5'-end of the GPAT1 transcript using GPAT1-specific reverse primers in exon 5. As shown in Fig. 2A, three transcript variants were obtained and were designated GPAT1 transcript variant 1 (GPAT1-V1), variant 2 (GPAT1-V2), and variant 3 (GPAT1-V3). GPAT1-V1 cDNA contained all three exon 1 sequences (1a, 1b and 1c), whereas GPAT1-V2 lacked the exon 1b sequence (Fig. 2A). The transcription

initiation site (+1) of GPAT1-V1 and V2 corresponded to the site that was shown in the previous report by Jerkins et al. [20] (see also Fig. 1B). GPAT1-V3 lacked exon 1a, and the transcription initiation site (+1) of this variant was located at the 13th upstream nucleotide of exon 1b in the mouse genome (Figs. 1B and 2A).

3.3. Expression of GPAT1 variants in mouse tissues and cultured cells

The expression patterns of each GPAT1 variant (GPAT1-V1, V2 and V3) were examined by RT-PCR analysis using specific primers (indicated in Table 1 and Fig. 2A) and RNA from various mouse tissues and cultured cells. As shown in Fig. 2B, all three variants were expressed in all tissues and cultured cells tested.

3.4. Translational efficiency of each GPAT1 variant

As shown in Fig. 2A, the protein-coding region of all GPAT1 mRNA variants begins at exon 1c, suggesting that an identical protein is produced from each of the three transcript variants. However, changes in the 5'-untranslated region of the mRNA might affect translational efficiency of the transcript as has been shown for other genes [35]. To examine the synthetic efficiency of proteins from each GPAT1 mRNA variant, *in vitro* protein production [35] was assessed for each variant. As shown in Fig. 2C, a coupled transcription/translation system yielded similar amounts of each GPAT1 protein variant. These levels were, however, lower compared to those produced from a GPAT1 cDNA without exons 1a and 1b (GPAT1 ORF alone; GPAT1-*myc*) (Fig. 2C), suggesting a role of exons 1a and 1b in attenuating GPAT1 protein production.

3.5. Identification of GPAT1 gene promoters

We have been unable to generate a full length DNA sequence of U11680 [20] from the mouse genome by PCR. However, 5'-flanking DNA fragments encoding nucleotides -1797 to +103 of the GPAT1-V1 (and V2) (promoter 1a; NCBI/GenBank accession number AB372190), and -2107 to +152 of the GPAT1-V3 (promoter 1b; NCBI/GenBank accession number AB372191) were generated by PCR based on the genome sequence information in NCBI/GenBank (Fig.

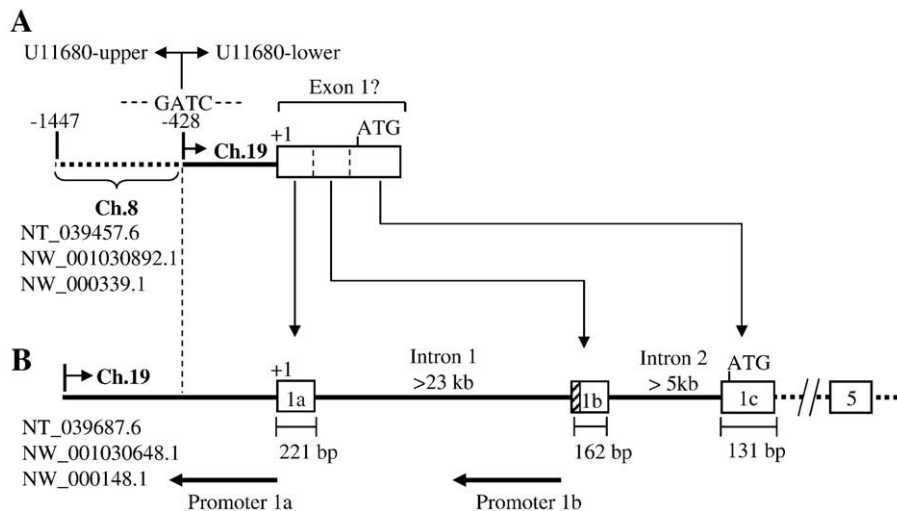


Fig. 1. Net genomic organization of the mouse GPAT1 gene. (A) Structure of the promoter region with putative exon 1 of the mouse GPAT1 gene according to the previous report by Jerkins et al. (NCBI/GenBank accession number U11680) [20]. Genome analysis revealed that the DNA region upstream from -428 [relative to the transcriptional initiation site (+1)] (termed U11680-upper) was mapped to contigs of Chromosome (Ch.) 8 (NT_039457.6, NW_001030892.1 or NW_000339.1), whereas a downstream sequence (U11680-lower) matched contigs of Ch. 19 (NT_039687.6, NW_001030648.1 or NW_000148.1). The border (GATC sequence) between the U11680-upper and -lower sequences is shown. Genome analysis further revealed that the DNA region downstream from +1 must be divided into three exon sequences (exons 1a, 1b, and 1c in panel B). (B) Net promoter regions and exon/intron organization of the mouse GPAT1 gene on Ch. 19. Boxes indicate the exons. The numbers of nucleotides in each exon or intron are shown. The diagonal box in panel B indicates a 5'-additional sequence upstream of exon 1b in the GPAT1-V3 variant (see Fig. 2A). The locations of promoters 1a and 1b for expression of the three GPAT1 transcript variants (GPAT1-V1, V2, and V3) (see Fig. 2A) are also shown in panel B. The locations of the translation initiation codon (ATG) in exon 1c are indicated in both panels.

Table 2
Nucleotide sequences at the exon–intron junctions of the mouse GPAT1 gene (from exons 1a to 1c)

Exon number	Splice acceptor	Splice donor
1a	–	ACATCAAGGATACAGg <u>tattt</u> gagcaactggga
1b	ttgtttcattc <u>ttctcag</u> AGCCTGGCAAAGAT	ATTAACAGGAGTTG <u>Ag</u> taagtataccggact
1c	tagtgcttattc <u>tctcag</u> CACATGGTTGGGACT	–

Exon and intron nucleotide sequences are shown in upper-case and lower-case letters, respectively. Donor and acceptor splice sites are underlined.

1B, [supplementary Fig. S1](#) and [S2](#)). Various 5'-segments for promoter 1a (from –1797, –789, –728, –325, and –86 to +103) and promoter 1b (from –2107, –809, –458, and –91 to +152) flanking each transcrip-

tional start site were inserted into a luciferase reporter plasmid, and transcriptional activities of these DNA regions were evaluated using HepG2 cells. As shown in [Fig. 3](#), basal promoter activity was regulated

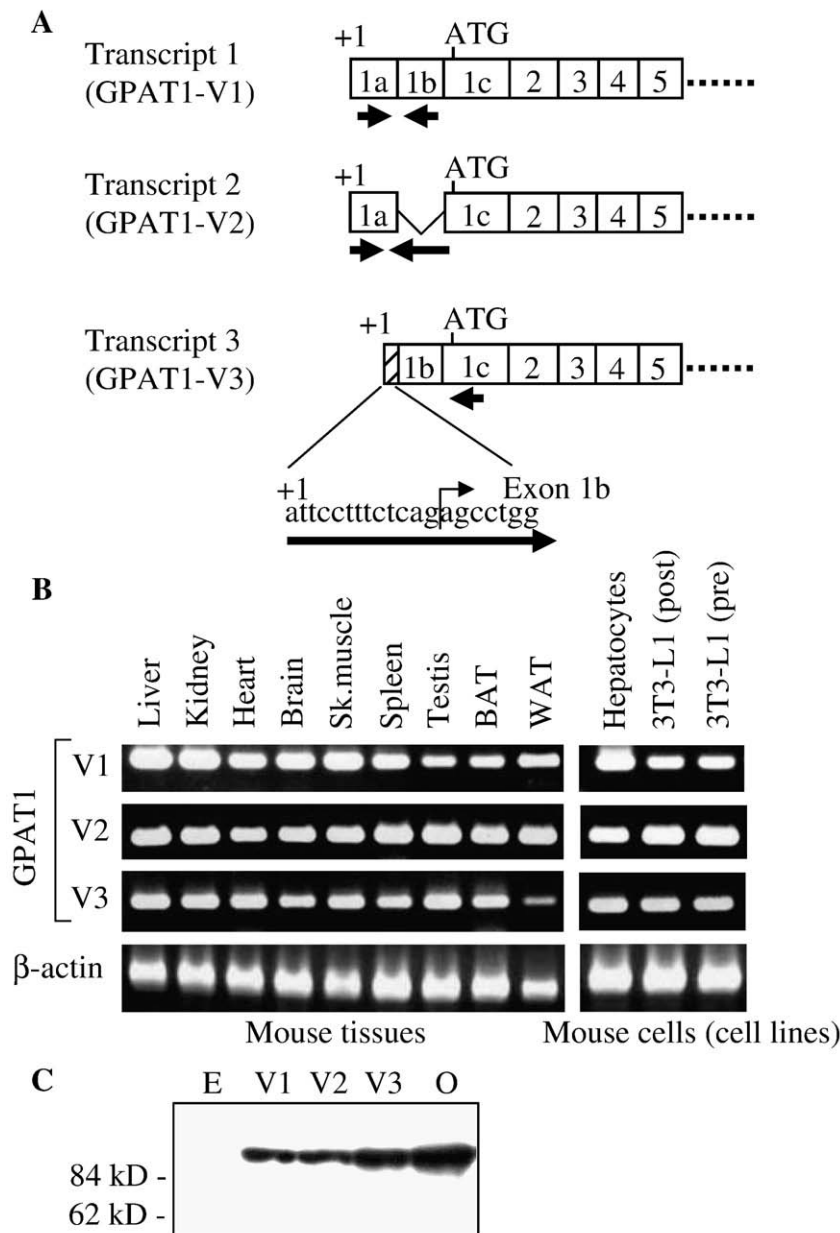


Fig. 2. The GPAT1 gene produces three transcript variants in mice. (A) Structures of the GPAT1 transcript variants (GPAT1-V1, V2 and V3) obtained by 5'-RACE analysis. Boxes indicate the exons. The transcription initiation sites (+1) and the translational initiation codon (ATG) are indicated. Arrows indicate the locations of the primers used for RT-PCR (panel B) as well as for the quantitative real-time RT-PCR analysis ([Fig. 9](#)). Primer sequences are shown in [Table 1](#). The diagonal box indicates 5'-additional sequence upstream of exon 1b in the GPAT1-V3 variant (see also [Fig. 1B](#)). (B) Expression of GPAT1 transcript variants in mouse tissues (C57BL/6 mice) and cultured cells. β -actin was used as an internal control. Sk. muscle: skeletal muscle (gastrocnemius). WAT: white adipose tissue (epididymal). BAT: brown adipose tissue. Hepatocytes: primary cultured hepatocytes. 3T3-L1 (pre): 3T3-L1 pre-adipocytes. 3T3-L1 (post): differentiated 3T3-L1 adipocytes. (C) Immunoblotting of the *in vitro*-translated myc-tagged proteins generated from the plasmids carrying each GPAT1 transcript variant cDNA (V1: GPAT1-V1-myc, V2: GPAT1-V2-myc, and V3: GPAT1-V3-myc). E: empty vector. The plasmid that carries GPAT1 cDNA but lacks exons 1a and 1b was used as an ORF alone control for the GPAT1 cDNA (o). Five microliters of the T_{NT}° product (see Materials and methods section) was electrophoresed on an SDS-polyacrylamide gel. Immunoblotting was performed using an anti-myc tag rabbit polyclonal antibody. Similar results were obtained from two independent experiments.

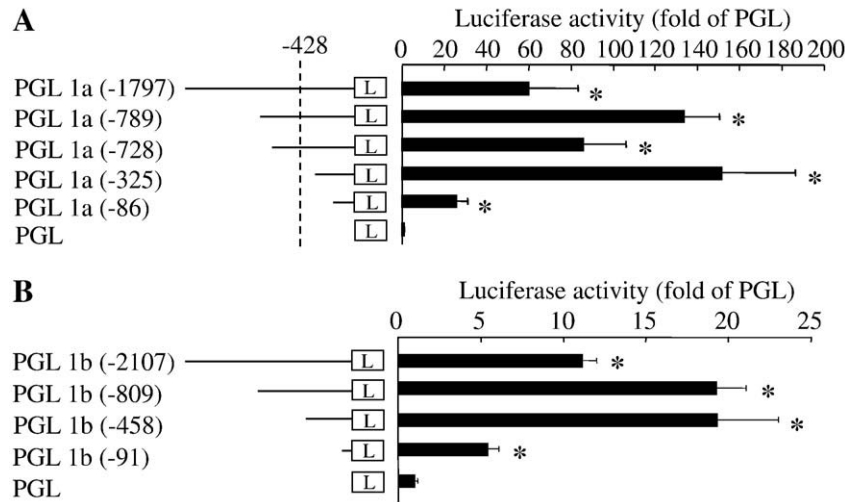


Fig. 3. Transcriptional activities of promoter 1a (A) and promoter 1b (B) of the mouse GPAT1 gene. HepG2 cells were transfected with one of the luciferase reporter plasmids [for promoter 1a: PGL 1a (-1797), (-789), (-728), (-325) or (-86), for promoter 1b: PGL 1b (-2107), (-809), (-458), or (-91)] and luciferase activities were evaluated at 48 h post-transfection. The location of the nucleotides of GATC at -428 (relative to the transcriptional start site in promoter 1a) is shown by a dotted line (see also Fig. 1). Luciferase activity was normalized for β -gal activity. A pGL3-basic vector (PGL) was used as a promoter-less control. Data are expressed as the means \pm SD of four culture wells (in a 24-well plate) in each group. The mean value for the promoter-less control (PGL) is designated as 1. * P <0.05 vs. PGL. L: luciferase. Similar results were obtained from three independent experiments.

by a region located between -86 and +103 for promoter 1a (Fig. 3A), and between -91 and +152 for promoter 1b (Fig. 3B). Additional DNA regions might act as modest enhancers (e.g. between -325 and -86 for promoter 1a) or silencers (e.g. between -728 and -325 for promoter 1a) for GPAT1 gene transcription (Fig. 3A and B).

3.6. Regulation of GPAT1 promoter activity by USF-1 and SREBP-1

Promoter 1a of the mouse GPAT1 gene contained an E-box (-324) and SRE-like sequences (SRE1: -186, SRE2: -170, and SRE3: -64 relative to the transcription start site) within the DNA region from

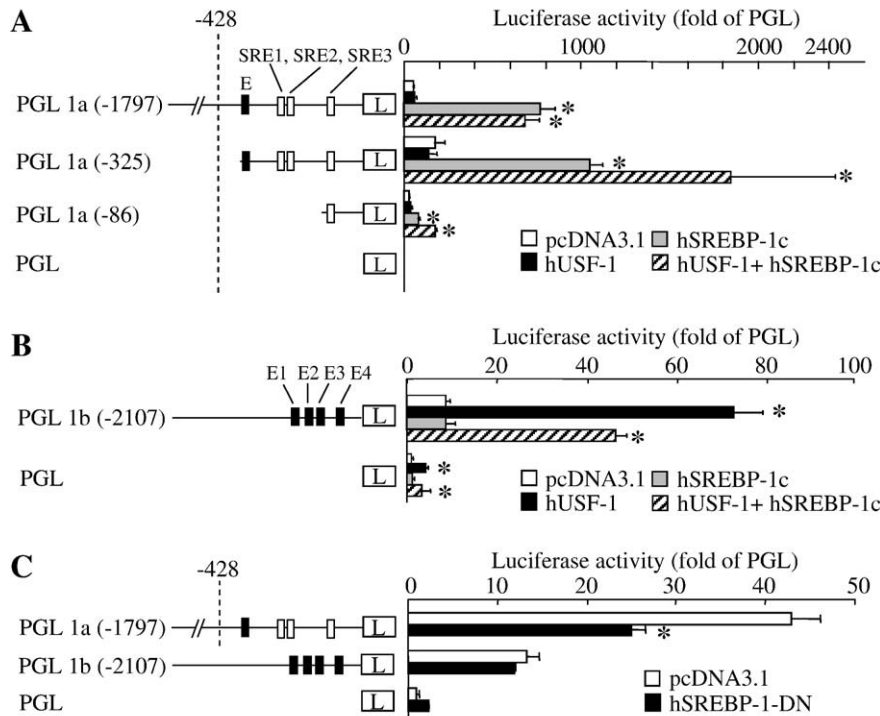


Fig. 4. Regulation of GPAT1 promoter activity by USF-1 and SREBP-1. (A) Regulation of promoter 1a activity by USF-1 and SREBP-1c. (B) Regulation of promoter 1b activity by USF-1 and SREBP-1c. (C) Regulation of promoters 1a and 1b activity by SREBP-1-DN. HepG2 cells were transfected with one of the luciferase reporter plasmids [for promoter 1a: PGL 1a (-1797), (-325), or (-86), for promoter 1b: PGL 1b (-2107)] together with an hUSF-1, hSREBP-1c or hSREBP-1-DN encoding or a non-coding (pcDNA3.1) plasmid. Luciferase activities were evaluated at 48 h post-transfection. A pGL3-basic vector (PGL) was used as a promoter-less control. Plasmids encoding hUSF-1 and hSREBP-1c were co-transfected in some cell cultures. The location of the nucleotides of GATC at -428 (relative to the transcription start site in promoter 1a) is shown by a dotted line (see also Fig. 1). The locations of E-boxes (E in panel A and E1 to E4 in panel B, and the same boxes in panel C) are shown by closed boxes. The locations of the SRE-like sequences (SRE1 to SRE3 in panel A and the same boxes in panel C) [21,23] in promoter 1a are indicated by open boxes. Luciferase activity was normalized for β -gal activity. Data are expressed as the means \pm SD of four culture wells (in a 24-well plate) in each group. The mean value for a promoter-less control (PGL) with an empty vector (pcDNA3.1) is designated as 1. * P <0.05 vs. empty vector (pcDNA3.1). L: luciferase. Similar results were obtained from two independent experiments.

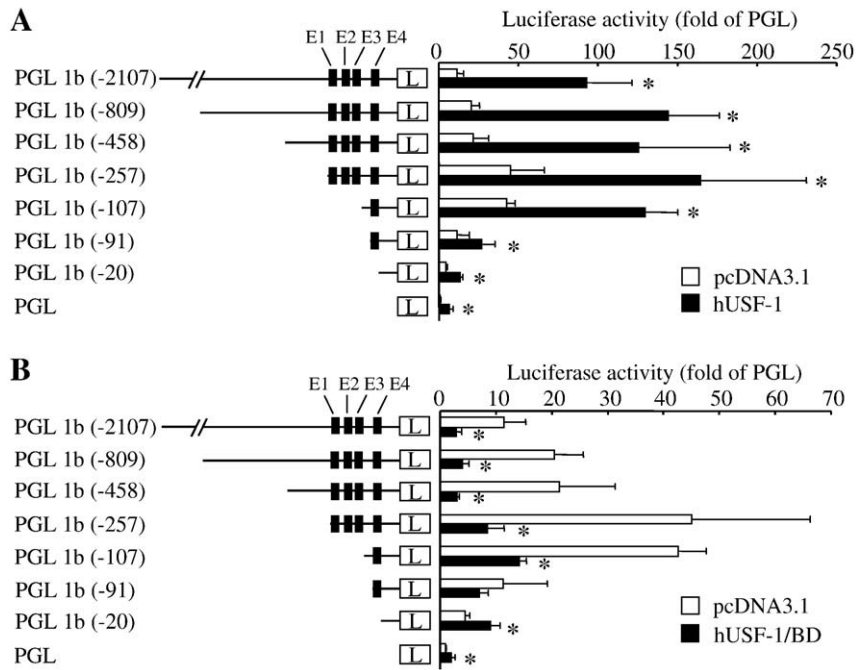


Fig. 5. Regulation of GPAT1 promoter 1b activity by hUSF-1 (A) and hUSF-1/BD (B). HepG2 cells were transfected with one of the luciferase reporter plasmids (as indicated) together with an hUSF-1 or an hUSF-1/BD-encoding or a non-coding (pcDNA3.1) plasmid. Luciferase activities were evaluated at 48 h post-transfection. A pGL3-basic vector (PGL) was used as a promoter-less control. The locations of four E-boxes (E1 to E4) are shown by closed boxes. Luciferase activity was normalized for β -gal activity. Data are expressed as the means \pm SD of four culture wells (in a 24-well plate) in each group. The mean value for a promoter-less control (PGL) with an empty vector (pcDNA3.1) is designated as 1. * P < 0.05 vs. empty vector (pcDNA3.1). L: luciferase. Similar results were obtained from two independent experiments.

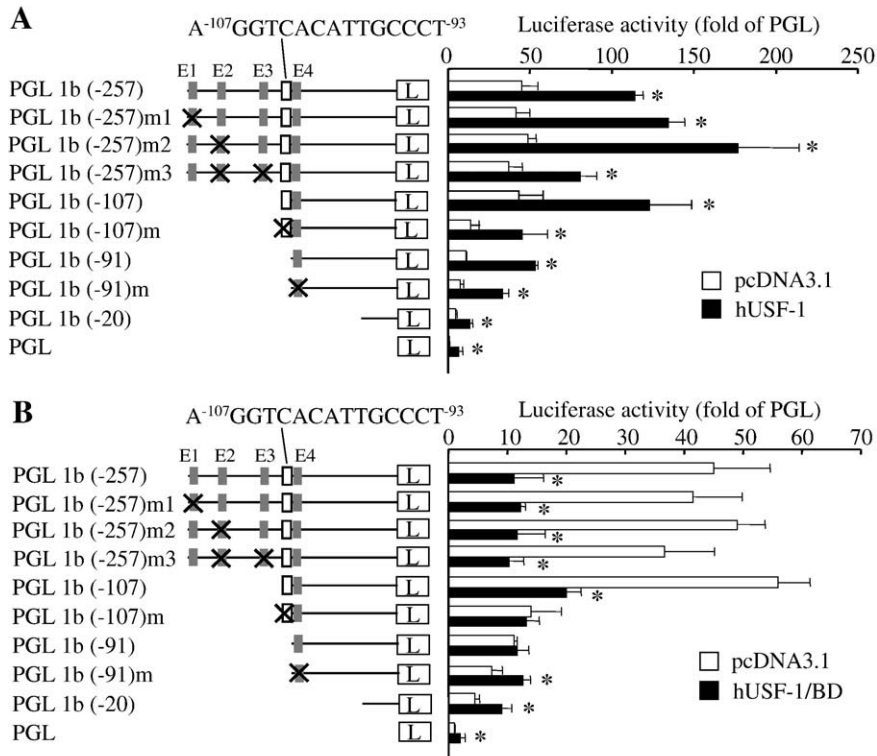


Fig. 6. Effect of site-directed mutagenesis in PGL 1b reporter plasmids on hUSF-1 (A) and hUSF-1/BD (B)-stimulated promoter 1b activity. HepG2 cells were transfected with one of the luciferase reporter plasmids (as indicated) together with an hUSF-1 or an hUSF-1/BD-encoding or a non-coding (pcDNA3.1) plasmid. Luciferase activities were evaluated at 48 h post-transfection. A pGL3-basic vector (PGL) was used as a promoter-less control. The locations of four E-boxes (E1 to E4) are shown by gray boxes. ERR-like sequence (A⁻¹⁰⁷GGTCACATTGCCCT⁻⁹³) located upstream of E4 is shown by open boxes. Site-directed mutagenesis resulted in the disruption of each motif (indicated by an X). Luciferase activity was normalized for β -gal activity. Data are expressed as the means \pm SD of four culture wells (in a 24-well plate) in each group. The mean value for a promoter-less control (PGL) with an empty vector (pcDNA3.1) is designated as 1. * P < 0.05 vs. empty vector (pcDNA3.1). L: luciferase. Similar results were obtained from two independent experiments.

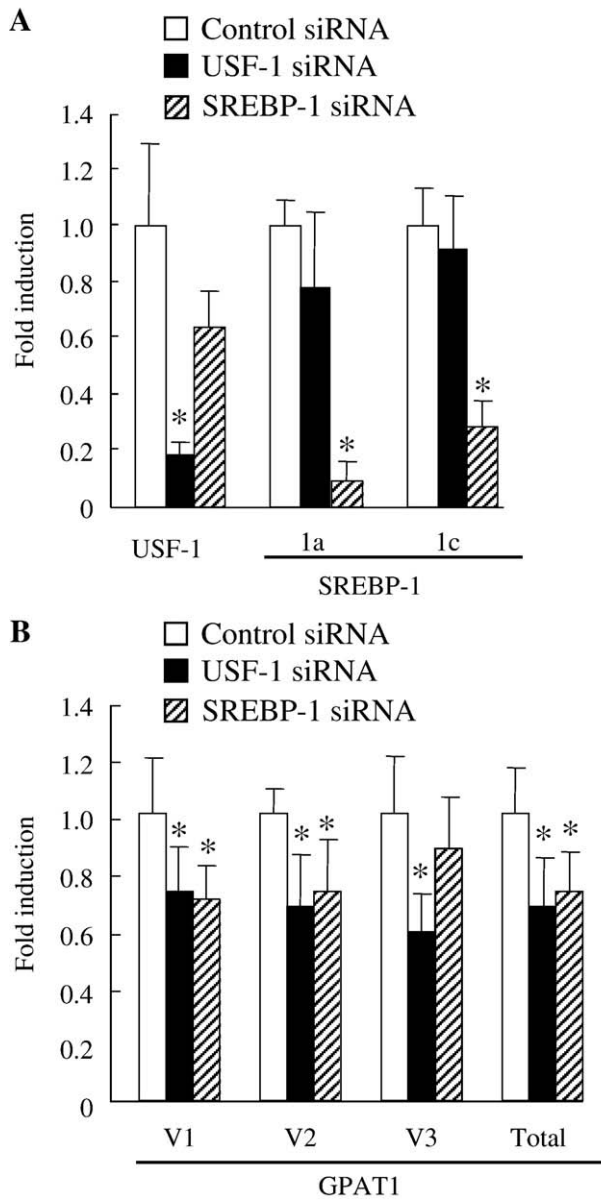


Fig. 8. Effect of RNAi against USF-1 or SREBP-1 on GPAT1 expression levels in mouse hepatocytes. Hepatocytes were transfected with siRNAs that target mouse USF-1 or mouse SREBP-1, or with control siRNA (scrambled sequence) 48 h prior to RNA extraction. (A) Endogenous mRNA expression levels of USF-1 and SREBP-1a/1c in siRNA-transfected mouse hepatocytes (quantitative real-time RT-PCR analysis). (B) Endogenous mRNA expression levels of each GPAT1 transcript variant [GPAT1-V1 (V1), V2 (V2), and V3 (V3)] in siRNA-transfected mouse hepatocytes (quantitative real-time RT-PCR analysis). Data are expressed as the means \pm SD of 5–6 culture dishes (6 cm dishes) in each group. Each mRNA expression level was normalized for the expression of 18S ribosomal RNA in each group. The mean value for the control siRNA group is designated as 1. * $P < 0.05$, when compared with control siRNA group.

promoter [42] did not affect the response of promoter 1b to exogenous hUSF-1/BD or hUSF-1 proteins in the present study (data not shown). Thus, we find no evidence of a weak USF-1-responsive domain in the core region of promoter 1b (located between -20 and $+152$). In this regard, if PGL 1b (-91) does not contain another USF-1-responsive sequence, hUSF-1/BD should increase its promoter activity. However, as shown in Fig. 5B, hUSF-1/BD actually failed to increase the luciferase activity of PGL 1b (-91). Thus, it is plausible that a nucleotide sequence located between -91 and -20 also responds to the dominant-negative effect of hUSF-1/BD. We hypothesize here that there is also a USF-1 responsive element located between -91 and

-20 . Our results additionally suggest that the three E-box-like sequences (E1 to E3) within the DNA region from -257 to -107 play no functional role in USF-1-mediated activation of promoter 1b. Point mutations in each E-box (E1 to E3) indeed did not significantly affect exogenous hUSF-1- or hUSF-1/BD-induced changes in promoter 1b activity (Fig. 6A and B).

3.8. Identification of the USF-1-responsive sequence in promoter 1b

We hypothesized that at least two USF-1-responsive sequences are located in promoter 1b (between -107 and -91 and between -91 and -20 relative to the transcription start site; see above). The nucleotide sequence positioned from -107 to -93 of promoter 1b was found to be an estrogen receptor response element (ERR; consensus sequence AGGTCAnnnTGACTT)-like sequence, A^{-107} GGTCACATTGCCT $^{-93}$ (Fig. 6A, B and supplementary Fig. S2), which could be recognized by USF proteins [43]. ERR (-like) sequences are known to be regulated by estrogens; however, a preliminary study failed to show an effect of β -estradiol (10^{-9} to 10^{-7} M) administration on promoter 1b activity in HepG2 cells (data not shown). This sequence also contained a non-canonical E-box sequence of C^{-103} ACATTG $^{-97}$ (CANNNTG). In addition, the nucleotide sequence from -80 to -75 (CACGTG) corresponded to E4, a fourth E-box sequence in promoter 1b (Fig. 6A and B). As shown in Fig. 6A and B, the basal promoter activity of PGL 1b (-107) and PGL 1b (-91) was decreased by disruption of ERR-like [PGL 1b (-107)m] and E4 [PGL 1b (-91)m] sequences, respectively. The hUSF-1-stimulated increase in luciferase activity was also less in PGL 1b (-107)m or PGL 1b (-91)m-transfected cells compared to PGL 1b (-107) or PGL 1b (-91) -transfected cells, respectively (Fig. 6A). In addition, exogenous overexpression of hUSF-1/BD failed to attenuate the luciferase activity of PGL 1b (-107)m-transfected HepG2 cells as was seen in the cells that were transfected with PGL 1b (-91) plasmid (Fig. 6B). In PGL 1b (-91)m-transfected cells, exogenous overexpression of hUSF-1/BD slightly increased luciferase activity as was seen in the PGL 1b (-20)m-transfected cells (Fig. 6B). Thus, ERR-like and E4 sequences in the promoter 1b of the GPAT1 gene can serve as targets for USF-1 action.

3.9. USF-1 binds to ERR-like and E4 sequences in the promoter 1b

To examine whether the USF-1 protein actually binds to the two USF-1-response elements (ERR-like and E4 sequence) in promoter 1b, EMSA was performed using *in vitro* translated hUSF-1 protein and

Table 3
Physical and biochemical characteristics of *db/m+* and *db/db* mice (8 weeks of age)

	<i>db/m+</i>		<i>db/db</i>	
	Fed	Fasted (48 h)	Fed	Fasted (48 h)
Body weight (g)	26.6 \pm 0.4	20.5 \pm 0.7*	40.4 \pm 1.8†	36.3 \pm 1.2**
Food intake	0.26 \pm 0.05	–	1.64 \pm 0.16†	–
[g/12 h (light)]	–	–	–	–
[g/12 h (dark)]	2.26 \pm 0.09	–	4.10 \pm 0.53#	–
[g/24 h]	2.53 \pm 0.04	–	5.74 \pm 0.69#	–
Epididymal fat (g)	0.36 \pm 0.07	0.18 \pm 0.03*	1.53 \pm 0.07†	1.54 \pm 0.10
Liver total lipid	38.5 \pm 6.0	176.6 \pm 99.1**	70.6 \pm 21.5#	150.0 \pm 22.9*
(μ g/mg tissue)	–	–	–	–
Liver TAG (μ g/mg tissue)	4.8 \pm 2.0	30.6 \pm 3.7*	18.0 \pm 2.9†	26.0 \pm 9.4
Blood glucose (mg/100 ml)	127.5 \pm 9.2	34.7 \pm 2.1*	432.7 \pm 48†	70.5 \pm 14.1*
Plasma insulin (ng/ml)	1.58 \pm 0.38	0.69 \pm 0.32**	5.40 \pm 1.13†	1.51 \pm 0.56*
Plasma TAG (mg/100 ml)	115.9 \pm 9.3	72.5 \pm 22.2**	373.9 \pm 24.7†	64.7 \pm 8.4*
Plasma total cholesterol	60.5 \pm 2.5	70.9 \pm 16.1	118.4 \pm 20.4†	78.8 \pm 4.9**
(mg/100 ml)	–	–	–	–
Plasma free fatty acid	0.10 \pm 0.03	0.78 \pm 0.28*	0.90 \pm 0.26†	0.94 \pm 0.29
(mEq/l)	–	–	–	–

* $P < 0.01$,

** $P < 0.05$, when compared with fed group.

† $P < 0.01$,

$P < 0.05$, when compared with *db/m+* group.

specific oligonucleotide probes or competitors shown in Fig. 7A. As shown in Fig. 7B, the formation of complexes between hUSF-1 and oligonucleotides carrying ERR-like sequence (oligo. A) or E4 sequence (oligo. B) was observed. The mutant probes Am and Bm failed to form complexes with hUSF-1 protein (Fig. 7B). The formation of a complex of hUSF-1 and oligo. A (or B) was inhibited in the presence of a non-labeled competitor A (or B) or an E-box positive sequence, but not in the presence of a non-labeled competitor Am (or Bm) (Fig. 7B). These results suggest that the USF-1 protein binds specifically to ERR-like sequence (−107 to −93) and E4 sequence (−80 to −75) located in promoter 1b of the GPAT1 gene.

3.10. Effect of RNAi against USF-1 or SREBP-1 on GPAT1 expression levels in mouse hepatocytes

As shown above (Fig. 4), USF-1 can activate promoters 1a and 1b, whereas SREBP-1 only activates promoter 1a of the GPAT1 gene. Hence,

the effects of a gene knockdown of endogenous USF-1 or SREBP-1 on the mRNA levels of the GPAT1 transcript variants (V1, V2, and V3) were examined in primary cultured mouse hepatocytes using specific siRNAs for each transcription factor. As shown in Fig. 8A, transfection of the cells with siRNA for USF-1 and SREBP-1 significantly decreased mRNA levels of endogenous USF-1 and SREBP-1 (both the 1a and 1c isoforms), respectively, when compared to cells transfected with non-specific control siRNAs. In this study, the mRNA levels of each GPAT1 transcript variant were measured (Fig. 8B). An siRNA for USF-1 significantly decreased mRNA levels of all three GPAT1 variants. However, knockdown of the endogenous SREBP-1 by siRNA significantly decreased mRNA levels of GPAT1-V1 and V2, but not of the V3 variant. The change in the mRNA levels of total GPAT1 was similar to that of the GPAT1-V1 or V2 levels (Fig. 8B). These results suggest that basal expression levels of USF-1 are necessary for expression of all three GPAT1 variants, i.e., it is necessary for the activity of both promoters in mouse hepatocytes. However, endogenous SREBP-1

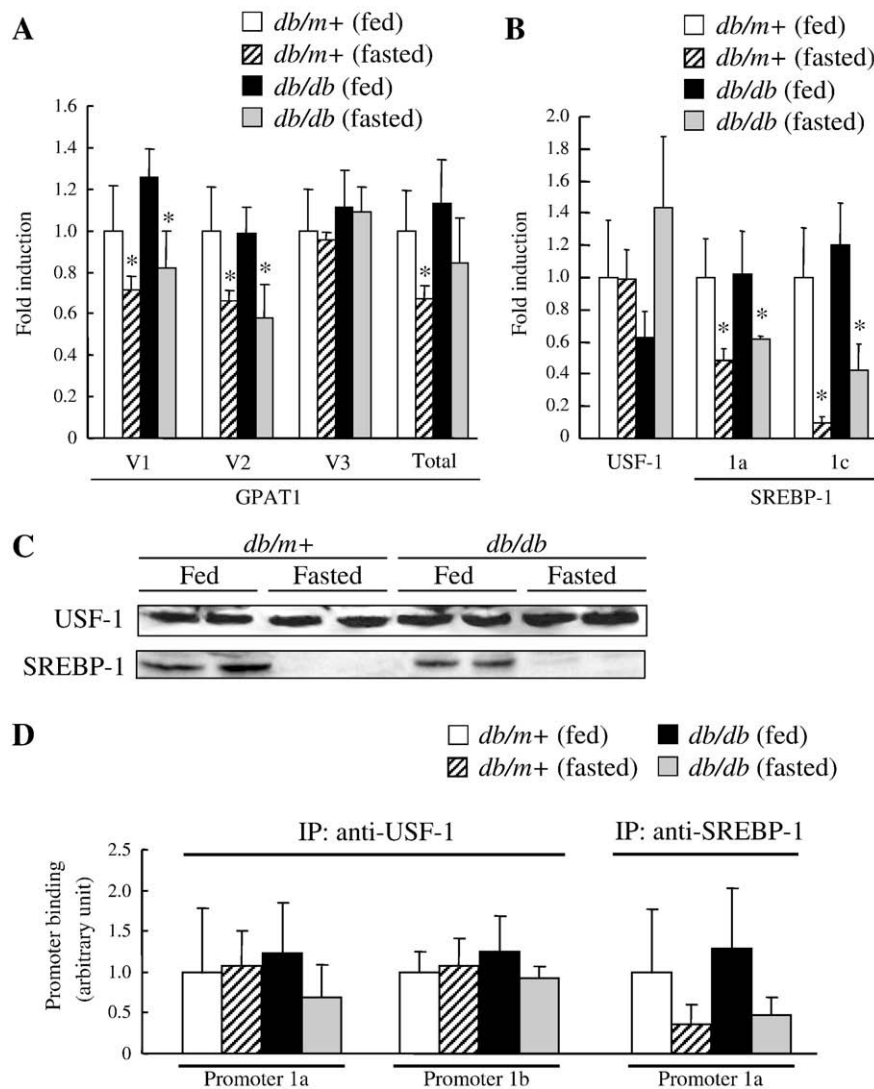


Fig. 9. Effect of fasting/feeding or obesity on the expression levels of GPAT1 in mouse liver. (A) mRNA expression levels of each GPAT1 variant or total GPAT1 in the liver of *db/m+* and *db/db* mice fed or fasted for 48 h (quantitative real-time RT-PCR analysis). (B) mRNA expression levels of USF-1, SREBP-1a, or SREBP-1c in the liver of *db/m+* and *db/db* mice fed or fasted for 48 h (quantitative real-time RT-PCR analysis). (C) Intracellular protein levels of USF-1 or SREBP-1 in the liver of *db/m+* and *db/db* mice fed or fasted for 48 h (Immunoblotting). Representative data from two mice in each group are shown. (D) Binding levels of USF-1 or SREBP-1 proteins to promoter 1a or promoter 1b of the GPAT1 gene in the liver of *db/m+* and *db/db* mice fed or fasted for 48 h (ChIP assay). Intracellular DNA–protein complexes were immunoprecipitated (IP) with the antibodies indicated and the amount of the precipitated DNA was quantified with quantitative real-time PCR analysis as described in Materials and methods section. Data in A, B, and D are expressed as the means \pm SD of four mice in each group. Each mRNA expression level was normalized for the expression of 18S ribosomal RNA in each group. The mean value for the fed *db/m+* group is designated as 1. * P < 0.05, when compared with the fed group.

regulates mRNA levels of GPAT1-V1 and V2 variants, i.e., it regulates only promoter 1a in these cells.

3.11. Involvement of USF-1 and SREBP-1 in nutritional regulation of GPAT1 gene expression *in vivo*

The expression levels of each GPAT1 gene variant and their relationships with the expression levels or promoter binding status of USF-1 and SREBP-1 were analyzed in the liver of obese *db/db* and non-obese *db/m+* (control) mice after fasting (48 h) or under *ad lib* feeding in this study. As shown in Table 3, *db/db* mice exhibited hyperphagia, hyperinsulinemia, and hyperglycemia as well as hyperlipidemia and attained a higher body weight as well as greater visceral fat mass compared to the normal *db/m+* mice. The amounts of total lipids and TAG in the liver were also higher in *db/db* mice than in normal controls (Table 3). Fasting of the animals in both groups decreased blood concentrations of glucose, insulin and TAG while also resulting in lipid accumulation in the liver (Table 3).

As shown in Fig. 9A, feeding increased GPAT1-V1 and V2 as well as total GPAT1 mRNA levels both in the control and *db/db* mice. GPAT1-V3 mRNA levels, however, did not respond to fasting/feeding manipulation in these mice (Fig. 9A). The obese and diabetic condition of the *db/db* mice had little effect on the expression levels of all GPAT1 variants tested (Fig. 9A). mRNA expression levels and intranuclear protein levels of USF-1 were not increased by feeding, whereas those of SREBP-1 (1a and 1c) were significantly up-regulated by feeding in both mouse genotypes (Fig. 9B and C). To examine the binding levels of USF-1 and SREBP-1 proteins to GPAT1 promoters, ChIP was performed using liver nuclear fractions isolated from the fasted and fed mice. As shown in Fig. 9D, the binding of USF-1 to promoter 1a or 1b of the GPAT1 gene was not affected by fasting/feeding manipulation or the obese and diabetic condition of the *db/db* mice. However, the binding of SREBP-1 to promoter 1a in the liver was increased slightly by feeding in both genotypes, although the hyperphagia seen in *db/db* mice did not further potentiate this binding (Fig. 9D).

4. Discussion

Here we have shown that three transcript variants (GPAT1-V1, V2, and V3) of the GPAT1 gene are expressed in the mouse. The transcription of both GPAT1-V1 and V2 mRNA is facilitated by the promoter 1a while the GPAT1-V3 variant is regulated by the downstream promoter 1b. Studies with experimental animals *in vivo* have suggested that the mRNA expression levels of the GPAT1-V1 and V2 variants were regulated by fasting and feeding whereas GPAT1-V3 mRNA levels were unchanged by nutritional manipulation (Fig. 9). The obese and diabetic condition of the *db/db* mice had little effect on the expression levels of all three GPAT1 variants (Fig. 9). The feeding-stimulated increases in the mRNA levels of total GPAT1 (V1+V2+V3) were similar to those of the V1 and V2 isoforms (Fig. 9), suggesting that promoter 1a activity is much greater than promoter 1b activity. The luciferase activity of transfected cells expressing promoter 1a sequence in the PGL3 vector (approximately 20 to 150 times higher than pGL3 vector alone) was indeed greater than that of the cells expressing promoter 1b sequence (approximately 5 to 20 times higher than pGL3 vector alone) in this study (Fig. 3). Thus, previously observed changes in the mRNA levels of GPAT1 under fasting/feeding manipulation [3] would appear to reflect changes in the expression levels of the V1 and V2 variants, but not of the V3 variant of this gene.

Our *in vitro* studies led us to conclude that USF-1 regulates the transcriptional activity of both promoter 1a and promoter 1b of the GPAT1 gene. However, mRNA expression levels, nuclear protein levels, and promoter (1a and 1b)-binding levels of USF-1 in our mouse livers were not increased by routine feeding *in vivo* (Fig. 9). Thus, USF-1 might not be involved in the feeding-induced stimulation of GPAT1 gene expression, although the basal promoter binding of the USF-1 protein is essential for the transcription of lipogenic genes including GPAT1 [23] (see also Fig. 8). On the other hand, mRNA expression levels and nuclear protein levels of SREBP-1 in mouse liver were significantly higher under fed conditions than fasting conditions (Fig. 9) as had been demonstrated in previous studies [44]. The feeding-

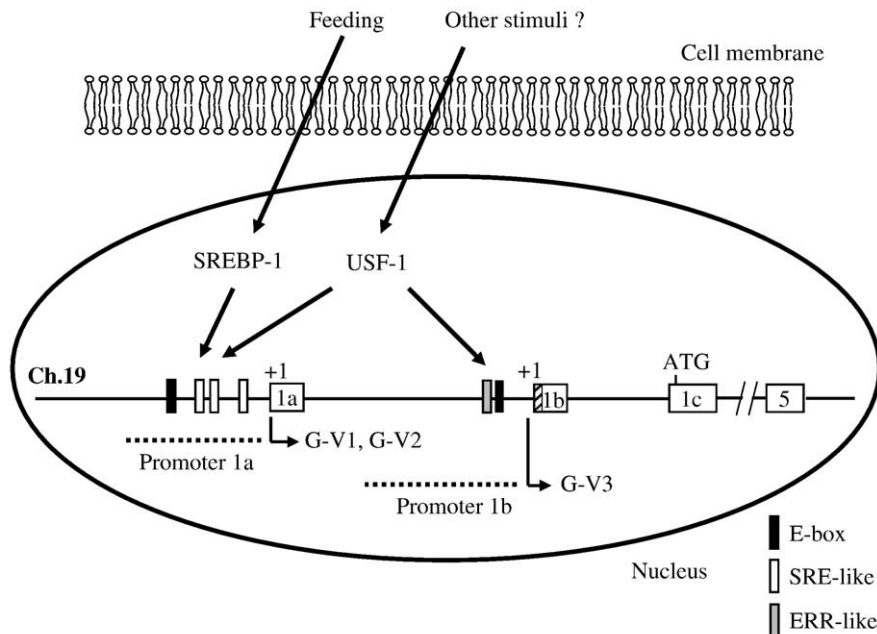


Fig. 10. Summarized model showing the regulation of hepatic GPAT1 gene expression *in vivo*. Transcription of the mouse GPAT1 gene is controlled by at least two promoters: promoter 1a and promoter 1b on Chromosome (Ch.) 19. Boxes indicate the exons. The transcription initiation sites (+1) and the translational initiation codon (ATG) are indicated. Feeding facilitates intranuclear accumulation of SREBP-1 which in turn binds to SRE-like sequences on promoter 1a of the GPAT1 gene. Activation of promoter 1a increases the transcription of V1 (G-V1) and V2 (G-V2) variants of the GPAT1 gene. USF-1 can associate with E-boxes (on promoter 1a or 1b) or ERR-like sequence (on promoter 1b); however, the expression levels as well as the binding levels of USF-1 to both promoters are not altered by fasting/feeding *in vivo*. Pathophysiological stimuli that regulate the transcription of GPAT1-V3 variant (G-V3) remain unclear.

induced rise in the binding levels of SREBP-1 to promoter 1a of the GPAT1 gene (Fig. 9) was almost identical to the previous results of Griffin et al. [23]. In the present study, exogenous overexpression of SREBP-1c stimulated, whereas overexpression of SREBP-1-DN inhibited, the activity of promoter 1a but not of promoter 1b in HepG2 cells (Fig. 4). An RNAi-induced knockdown of endogenous SREBP-1 actually decreased expression of GPAT1-V1 and V2, but not of GPAT1-V3 mRNA levels in mouse hepatocytes (Fig. 8). Thus, SREBP-1 could play a significant role in feeding-induced activation of promoter 1a, facilitating GPAT1 gene expression in the liver (Fig. 10). In contrast, the downstream promoter 1b which lacks SRE (-like) sequence would not respond to fasting or feeding *in vivo* (Fig. 10).

The molecular stimuli that facilitate SREBP-1-dependent GPAT1 transcription remain unclear. Several previous studies have suggested that insulin may be a critical factor mediating the postprandial increase in lipogenic gene expression [3,38,45,46]. Hepatic GPAT1 gene expression has been reported to be increased following an insulin injection in animals, while it is decreased in streptozotocin (STZ)-induced type I diabetic liver [3]. Thus, the observed rise in the plasma insulin levels under fed conditions (Table 3) might reflect an involvement of insulin in the feeding-stimulated rise in hepatic GPAT1 mRNA levels. However, we have previously demonstrated that feeding itself even in non-diabetic mice is not sufficient to activate downstream signaling molecules (e.g. Akt/protein kinase B and glycogen synthase kinase-3 α/β) of insulin action in the liver [26]. Although we and others have shown a slight induction of SREBP-1 mRNA expression by a supra-physiological concentration of insulin (100 nM) *in vitro* [28,47], our preliminary experiments revealed that the insulin at this concentration was not sufficient to induce GPAT1 gene expression in primary mouse hepatocytes (M. Yoshida and N. Harada, unpublished data). A recent study of transgenic mice expressing a transgene with an SREBP-1c promoter-driven reporter clearly demonstrated an insulin-independent refeeding response of SREBP-1 gene transcription *in vivo* [48]. Thus, changes in insulin levels during routine feeding in mice may not be sufficient to elevate GPAT1 gene expression in the liver. An alternative hypothesis is the possibility that glucose could stimulate GPAT1 gene expression. Recently, the liver X receptors (LXRs) have been identified as novel glucose sensors in mammalian cells [49], although another study failed to show this effect [50]. SREBP-1c expression is known to be one of the targets of LXR action [50] and it was indeed slightly elevated in liver cells in a high glucose environment [28,51]. Given the fact that feeding of LXR α/β knockout mice failed to increase GPAT1 gene expression in the liver [50], a hyperglycemic effect on the feeding-stimulated increase of hepatic GPAT1 gene expression was speculated. However, hepatic GPAT1 mRNA levels were not increased even in the presence of hyperglycemia in our *db/db* mice (Fig. 9 and Table 3) or in STZ-induced type I diabetic mice [3]. A high glucose environment (25 mM) indeed failed to potentiate GPAT1 promoter 1a or 1b activity in our preliminary luciferase assays (data not shown). Thus, the involvement of a high glucose environment in the regulation of GPAT1 gene expression in the liver remains to be clarified. Further investigation is needed to elucidate the molecular mechanisms required for up-regulation of hepatic GPAT1 gene expression during routine feeding.

It should be noted here that fasting caused the accumulation of lipids, including triacylglycerol, in the liver (Table 3). The increase in intrahepatic lipids during fasting has been described to be mainly due to an increased influx of free fatty acids into the liver [52]. Lee et al. [53] has demonstrated using a knockout mouse that peroxisome proliferator-activated receptor- α (PPAR- α), a well known transcription factor which mediates transcription of lipolytic genes [54], plays an important role in maintaining hepatic lipid profiles during fasting. In the upstream region of promoter 1a of the GPAT1 gene, i.e., in the sequence upstream of -428 in promoter 1a, a PPAR-responsive element (consensus AGGTCAAnAGGTCA)-like sequence 5'-AGGTCA-

CAGGGCA-3' at the nucleotide position -747 to -735 (relative to the transcriptional start site) was found (supplementary Fig. S1). In this motif, the hexamers AGGTCA were arranged as direct repeats with an interspacing of 1 bp [termed direct repeat 1 (DR1)] [55]. A heterodimer of PPAR α and retinoid X receptor (RXR) binds to this motif and regulates target gene expression [55]. However, when 'C' is an intervening base in a DR1, the binding intensity of the PPAR α /RXR α heterodimer to DR1 largely decreases [55]. The DR1-like sequence identified in promoter 1a of the GPAT1 gene has 'C' as an intervening base between two AGGTCA-like hexamers. Thus, our preliminary luciferase assays in HepG2 cells did not show a response of this motif to either exogenous overexpression of PPAR α /RXR α or to the selective PPAR α ligand Wy-14643 (up to 100 μ M) (data not shown).

Recently, Aneja et al. have identified two promoters of the rat GPAT1 gene [56]. One promoter (they termed this the "distal promoter") matches the mouse promoter 1a, while the other (termed the "proximal promoter") does not match mouse promoter 1b, but is located downstream of the second exon (which corresponds to exon 1c in mouse) of the rat GPAT1 gene [56]. Nutritional regulation of hepatic GPAT1 expression in both the mouse and the rat was mainly controlled by the activity of promoter 1a [the distal promoter in the rat [56]]. Future studies should be undertaken to identify the stimuli that target the remaining promoters in mammalian cells. Elucidation of alternative regulatory systems for promoter selectivity of GPAT1 gene would help to understand the molecular basis of glycerophospholipid synthesis in various pathophysiological conditions.

Acknowledgements

This study was supported in part by the 21st-Century COE project, Human Nutrition Science on Stress Control, Tokushima, Japan, and by a Grant-in-Aid for Scientific Research from the Ministry of Education, Science, Sports, and Culture and Technology, Japan to Nagakatsu Harada (20790496).

Appendix A. Supplementary data

Supplementary data associated with this article can be found, in the online version, at doi:10.1016/j.bbali.2008.09.005.

References

- [1] M.R. Gonzalez-Baró, T.M. Lewin, R.A. Coleman, Regulation of triglyceride metabolism. II. Function of mitochondrial GPAT1 in the regulation of triacylglycerol biosynthesis and insulin action, *Am. J. Physiol. Gastrointest. Liver Physiol.* 292 (2007) 1195–1199.
- [2] L.K. Dircks, H.S. Sul, Mammalian mitochondrial glycerol-3-phosphate acyltransferase, *Biochim. Biophys. Acta* 1348 (1997) 17–26.
- [3] D.H. Shin, J.D. Paulauskis, N. Moustaid, H.S. Sul, Transcriptional regulation of p90 with sequence homology to *Escherichia coli* glycerol-3-phosphate acyltransferase, *J. Biol. Chem.* 266 (1991) 23834–23839.
- [4] N. Harada, S. Hara, M. Yoshida, T. Zenitani, K. Mawatari, M. Nakano, A. Takahashi, T. Hosaka, K. Yoshimoto, Y. Nakaya, Molecular cloning of a murine glycerol-3-phosphate acyltransferase-like protein 1 (xGPAT1), *Mol. Cell. Biochem.* 297 (2007) 41–51.
- [5] S. Wang, D.P. Lee, N. Gong, N.M. Schwerbrock, D.G. Mashek, M.R. Gonzalez-Baró, C. Stapleton, L.O. Li, T.M. Lewin, R.A. Coleman, Cloning and functional characterization of a novel mitochondrial N-ethylmaleimide-sensitive glycerol-3-phosphate acyltransferase (GPAT2), *Arch. Biochem. Biophys.* 465 (2007) 347–358.
- [6] J. Cao, J.L. Li, D. Li, J.F. Tobin, R.E. Gimeno, Molecular identification of microsomal acyl-CoA:glycerol-3-phosphate acyltransferase, a key enzyme in *de novo* triacylglycerol synthesis, *Proc. Natl. Acad. Sci. U. S. A.* 103 (2006) 19695–19700.
- [7] C.A. Nagle, L. Vergnes, H. Dejong, S. Wang, T.M. Lewin, K. Reue, R.A. Coleman, Identification of a novel sn-glycerol-3-phosphate acyltransferase isoform, GPAT4, as the enzyme deficient in *Apat6*^{-/-} mice, *J. Lipid Res.* 49 (2008) 823–831.
- [8] Y.Q. Chen, M.S. Kuo, S. Li, H.H. Bui, P.D.A. Eake, P.E. Sanders, S.J. Thibodeaux, S. Chu, Y.W. Qian, Y. Zhao, D.S. Bredt, D.E. Moller, R.J. Konrad, A.P. Beigneux, S.G. Young, G. Cao, AGPAT6 is a novel microsomal glycerol-3-phosphate acyltransferase, *J. Biol. Chem.* 283 (2008) 10048–10057.
- [9] T.M. Lewin, D.A. Granger, J.H. Kim, R.A. Coleman, Regulation of mitochondrial sn-glycerol-3-phosphate acyltransferase activity: response to feeding status is unique in various rat tissues and is discordant with protein expression, *Arch. Biochem. Biophys.* 396 (2001) 119–127.

- [10] R.A. Coleman, T.M. Lewin, D.M. Muoio, Physiological and nutritional regulation of enzymes of triacylglycerol synthesis, *Annu. Rev. Nutr.* 20 (2000) 77–103.
- [11] D. Linden, L. William-Olsson, M. Rhedin, A.K. Asztely, J.C. Clapham, S. Schreyer, Overexpression of mitochondrial GPAT in rat hepatocytes leads to decreased fatty acid oxidation and increased glycerolipid biosynthesis, *J. Lipid Res.* 45 (2004) 1279–1288.
- [12] R.A. Igal, S. Wang, M. Gonzalez-Baro, R.A. Coleman, Mitochondrial glycerol phosphate acyltransferase directs the incorporation of exogenous fatty acids into triacylglycerol, *J. Biol. Chem.* 276 (2001) 42205–42212.
- [13] D. Lindén, L. William-Olsson, A. Ahnmark, K. Ekroos, C. Hallberg, H.P. Sjögren, B. Becker, L. Svensson, J.C. Clapham, J. Oscarsson, S. Schreyer, Liver-directed overexpression of mitochondrial glycerol-3-phosphate acyltransferase results in hepatic steatosis, increased triacylglycerol secretion and reduced fatty acid oxidation, *FASEB J.* 20 (2006) 434–443.
- [14] L.E. Hammond, P.A. Gallagher, S. Wang, S. Hiller, K.D. Kluckman, E.L. Posey-Marcos, N. Maeda, R.A. Coleman, Mitochondrial glycerol-3-phosphate acyltransferase-deficient mice have reduced weight and liver triacylglycerol content and altered glycerolipid fatty acid composition, *Mol. Cell. Biol.* 22 (2002) 8204–8214.
- [15] H. Xu, D. Wilcox, P. Nguyen, M. Voorbach, T. Suhar, S.J. Morgan, W.F. An, L. Ge, J. Green, Z. Wu, R.E. Gimeno, R. Reilly, P.B. Jacobson, C.A. Collins, K. Landschulz, T. Surowy, Hepatic knockdown of mitochondrial GPAT1 in *ob/ob* mice improves metabolic profile, *Biochem. Biophys. Res. Commun.* 349 (2006) 439–448.
- [16] C.A. Nagle, J. An, M. Shiota, T.P. Torres, G.W. Cline, Z.X. Liu, S. Wang, R.L. Catlin, G.I. Shulman, C.B. Newgard, R.A. Coleman, Hepatic overexpression of glycerol-sn-3-phosphate acyltransferase 1 in rats causes insulin resistance, *J. Biol. Chem.* 282 (2007) 14807–14815.
- [17] E.R. Thureson, Inhibition of glycerol-3-phosphate acyltransferase as a potential treatment for insulin resistance and type 2 diabetes, *Curr. Opin. Investig. Drugs* 5 (2004) 411–418.
- [18] B. Ganesh-Bhat, P. Wang, J.H. Kim, T.M. Black, T.M. Lewin, F.T. Fiedorek Jr., R.A. Coleman, Rat sn-glycerol-3-phosphate acyltransferase: molecular cloning and characterization of the cDNA and expressed protein, *Biochim. Biophys. Acta* 1439 (1999) 415–423.
- [19] C.L. Welch, Y.R. Xia, P.A. Edwards, A.J. Lusic, J. Ericsson, Assignment of Gpm to distal mouse Chromosome 19 by linkage analysis, *Mamm. Genome* 9 (1998) 93.
- [20] A.A. Jerkins, W.R. Liu, S. Lee, H.S. Sul, Characterization of the murine mitochondrial glycerol-3-phosphate acyltransferase promoter, *J. Biol. Chem.* 270 (1995) 1416–1421.
- [21] J. Ericsson, S.M. Jackson, J.B. Kim, B.M. Spiegelman, P.A. Edwards, Identification of glycerol-3-phosphate acyltransferase as an adipocyte determination and differentiation factor 1- and sterol regulatory element-binding protein-responsive gene, *J. Biol. Chem.* 272 (1997) 7298–7305.
- [22] P.J. Espenshade, SREBPs: sterol-regulated transcription factors, *J. Cell Sci.* 119 (2006) 973–976.
- [23] M.J. Griffin, R.H. Wong, N. Pandya, H.S. Sul, Direct interaction between USF and SREBP-1c mediates synergistic activation of the fatty-acid synthase promoter, *J. Biol. Chem.* 282 (2007) 5453–5467.
- [24] J. Folch, M. Lees, G.H. Sloane, A simple method for the isolation and purification of total lipides from animal tissues, *J. Biol. Chem.* 226 (1957) 497–509.
- [25] J.K. Drackley, J.J. Veenhuizen, M.J. Richard, J.W. Young, Metabolic changes in blood and liver of dairy cows during either feed restriction or administration of 1,3-butanediol, *J. Dairy Sci.* 74 (1991) 4254–4264.
- [26] R. Matsushima, N. Harada, N.J. Webster, Y.M. Tsutsumi, Y. Nakaya, Effect of TRB3 on insulin and nutrient-stimulated hepatic p70 S6 kinase activity, *J. Biol. Chem.* 281 (2006) 29719–29729.
- [27] M.P. Weiner, G.L. Costa, W. Schoettlin, J. Cline, E. Mathur, J.C. Bauer, Site-directed mutagenesis of double-stranded DNA by the polymerase chain reaction, *Gene* 151 (1994) 119–123.
- [28] N. Harada, H. Yonemoto, M. Yoshida, H. Yamamoto, Y. Yin, A. Miyamoto, A. Hattori, Q. Wu, T. Nakagawa, M. Nakano, K. Teshigawara, K. Mawatari, T. Hosaka, A. Takahashi, Y. Nakaya, Alternative splicing produces a constitutively active form of human SREBP-1, *Biochem. Biophys. Res. Commun.* 368 (2008) 820–826.
- [29] T. Saito, T. Oishi, K. Yanai, Y. Shimamoto, A. Fukamizu, Cloning and characterization of a novel splicing isoform of USF1, *Int. J. Mol. Med.* 12 (2003) 161–167.
- [30] D. Botolin, D.B. Jump, Selective proteolytic processing of rat hepatic sterol regulatory element binding protein-1 (SREBP-1) and SREBP-2 during postnatal development, *J. Biol. Chem.* 278 (2003) 6959–6962.
- [31] Y. Taketani, H. Segawa, M. Chikamori, K. Morita, K. Tanaka, S. Kido, H. Yamamoto, Y. Iemori, S. Tatsumi, N. Tsugawa, T. Okano, T. Kobayashi, K. Miyamoto, E. Takeda, Regulation of type II renal Na⁺-dependent inorganic phosphate transporters by 1,25-dihydroxyvitamin D₃. Identification of a vitamin D-responsive element in the human NAPI-3 gene, *J. Biol. Chem.* 273 (1998) 14575–14581.
- [32] L.A. deGraffenried, T.A. Hopp, A.J. Valente, R.A. Clark, S.A. Fuqua, Regulation of the estrogen receptor alpha minimal promoter by Sp1, USF-1 and ERalpha, *Breast Cancer Res. Treat.* 85 (2004) 111–120.
- [33] M.J. Latasa, M.J. Griffin, Y.S. Moon, C. Kang, H.S. Sul, Occupancy and function of the -150 sterol regulatory element and -65 E-box in nutritional regulation of the fatty acid synthase gene in living animals, *Mol. Cell. Biol.* 23 (2003) 5896–5907.
- [34] C. Shin, J.L. Manley, Cell signalling and the control of pre-mRNA splicing, *Nat. Rev. Mol. Cell Biol.* 5 (2004) 727–738.
- [35] L.K. Larsen, E.Z. Amri, S. Mandrup, C. Pacot, K. Kristiansen, Genomic organization of the mouse peroxisome proliferator-activated receptor beta/delta gene: alternative promoter usage and splicing yield transcripts exhibiting differential translational efficiency, *Biochem. J.* 366 (2002) 767–775.
- [36] M. Amemiya-Kudo, H. Shimano, A.H. Hasty, N. Yahagi, T. Yoshikawa, T. Matsuzaka, H. Okazaki, Y. Tamura, Y. Iizuka, K. Ohashi, J. Osuga, K. Harada, T. Gotoda, R. Sato, S. Kimura, S. Ishibashi, N. Yamada, Transcriptional activities of nuclear SREBP-1a, -1c, and -2 to different target promoters of lipogenic and cholesterologenic genes, *J. Lipid Res.* 43 (2002) 1220–1235.
- [37] H. Shimano, Sterol regulatory element-binding proteins (SREBPs): transcriptional regulators of lipid synthetic genes, *Prog. Lipid Res.* 40 (2001) 439–452.
- [38] H.S. Sul, D. Wang, Nutritional and hormonal regulation of enzymes in fat synthesis: studies of fatty acid synthase and mitochondrial glycerol-3-phosphate acyltransferase gene transcription, *Annu. Rev. Nutr.* 18 (1998) 331–351.
- [39] R. Sato, J. Yang, X. Wang, M.J. Evans, Y.K. Ho, J.L. Goldstein, M.S. Brown, Assignment of the membrane attachment, DNA binding, and transcriptional activation domains of sterol regulatory element-binding protein-1 (SREBP-1), *J. Biol. Chem.* 269 (1994) 17267–17273.
- [40] G.A. Breen, E.M. Jordan, Upstream stimulatory factor 2 stimulates transcription through an initiator element in the mouse cytochrome c oxidase subunit Vb promoter, *Biochim. Biophys. Acta* 1517 (2000) 119–127.
- [41] J.E. Butler, J.T. Kadonaga, The RNA polymerase II core promoter: a key component in the regulation of gene expression, *Genes Dev.* 16 (2002) 2583–2592.
- [42] H. Du, A.L. Roy, R.G. Roeder, Human transcription factor USF stimulates transcription through the initiator elements of the HIV-1 and the Ad-ML promoters, *EMBO J.* 12 (1993) 501–511.
- [43] M. Kaling, T. Weimar-Ehl, M. Kleinhans, G.U. Ryffel, Transcription factors different from the estrogen receptor stimulate in vitro transcription from promoters containing estrogen response elements, *Mol. Cell. Endocrinol.* 69 (1990) 167–178.
- [44] J.D. Horton, Y. Bashmakov, I. Shimomura, H. Shimano, Regulation of sterol regulatory element binding proteins in livers of fasted and refed mice, *Proc. Natl. Acad. Sci. U. S. A.* 95 (1998) 5987–5992.
- [45] J.D. Paulauskis, H.S. Sul, Hormonal regulation of mouse fatty acid synthase gene transcription in liver, *J. Biol. Chem.* 264 (1989) 574–577.
- [46] C. Mounier, B.I. Posner, Transcriptional regulation by insulin: from the receptor to the gene, *Can. J. Physiol. Pharmacol.* 84 (2006) 713–724.
- [47] M. Matsumoto, W. Ogawa, K. Teshigawara, H. Inoue, K. Miyake, H. Sakaue, M. Kasuga, Role of the insulin receptor substrate 1 and phosphatidylinositol 3-kinase signaling pathway in insulin-induced expression of sterol regulatory element binding protein 1c and glucokinase genes in rat hepatocytes, *Diabetes* 51 (2002) 1672–1680.
- [48] Y. Takeuchi, N. Yahagi, Y. Nakagawa, T. Matsuzaka, R. Shimizu, M. Sekiya, Y. Iizuka, K. Ohashi, T. Gotoda, M. Yamamoto, R. Nagai, T. Kadowaki, N. Yamada, J. Osuga, H. Shimano, *In vivo* promoter analysis on refeeding response of hepatic sterol regulatory element-binding protein-1c expression, *Biochem. Biophys. Res. Commun.* 363 (2007) 329–335.
- [49] N. Mitro, P.A. Mak, L. Vargas, C. Godio, E. Hampton, V. Molteni, A. Kreusch, E. Saez, The nuclear receptor LXR is a glucose sensor, *Nature* 445 (2007) 219–223.
- [50] P.D. Denechaud, P. Bossard, J.M. Lobaccaro, L. Millatt, B. Staels, J. Girard, C. Postic, ChREBP, but not LXRs, is required for the induction of glucose-regulated genes in mouse liver, *J. Clin. Invest.* 118 (2008) 956–964.
- [51] A.H. Hasty, H. Shimano, N. Yahagi, M. Amemiya-Kudo, S. Perrey, T. Yoshikawa, J. Osuga, H. Okazaki, Y. Tamura, Y. Iizuka, F. Shionoiri, K. Ohashi, K. Harada, T. Gotoda, R. Nagai, S. Ishibashi, N. Yamada, Sterol regulatory element-binding protein-1 is regulated by glucose at the transcriptional level, *J. Biol. Chem.* 275 (2000) 31069–31077.
- [52] V. van Ginneken, E. Verhey, R. Poelmann, R. Ramakers, K.W. van Dijk, L. Ham, P. Voshol, L. Havekes, M. Van Eck, J. van der Greef, Metabolomics (liver and blood profiling) in a mouse model in response to fasting: a study of hepatic steatosis, *Biochim. Biophys. Acta* 1771 (2007) 1263–1270.
- [53] S.S. Lee, W.Y. Chan, C.K. Lo, D.C. Wan, D.S. Tsang, W.T. Cheung, Requirement of PPARalpha in maintaining phospholipid and triacylglycerol homeostasis during energy deprivation, *J. Lipid Res.* 45 (2004) 2025–2037.
- [54] S. Yu, S. Rao, J.K. Reddy, Peroxisome proliferator-activated receptors, fatty acid oxidation, steatohepatitis and hepatocarcinogenesis, *Curr. Mol. Med.* 3 (2003) 561–572.
- [55] H. Castelein, P.E. Declercq, M. Baes, DNA binding preferences of PPAR alpha/RXR alpha heterodimers, *Biochem. Biophys. Res. Commun.* 233 (1997) 91–95.
- [56] K.K. Aneja, P. Guha, R.Y. Shilpi, S. Chakraborty, L.M. Schramm, D. Haldar, The presence of distal and proximal promoters for rat mitochondrial glycerol-3-phosphate acyltransferase, *Arch. Biochem. Biophys.* 470 (2008) 35–43.